ELSEVIER

Ceramics International 28 (2002) 349–354

CERAMICS INTERNATIONAL

www.elsevier.com/locate/ceramint

# Preparation and characterization of doped sol–gel zirconia films

Weimin Liu*, Yunxia Chen, Chengfeng Ye, Pingyu Zhang

*State Key Laboratory of Solid Lubrication, Lanzhou Institute of Chemical Physics, Chinese Academy of Sciences, Lanzhou 730000, China*

Received 28 May 2001; received in revised form 23 July 2001; accepted 2 September 2001

**Abstract**

Highly oriented $CeO_2$-, $Y_2O_3$- and MgO-doped $ZrO_2$ thin films have been successfully prepared by a sol-gel process by dip-coating an ethanol solution of zirconium oxychloride octahydrate and the corresponding inorganic dopants. The doped $ZrO_2$ films contain only the zirconia tetragonal phase and show nano-scale morphology. Under low load, doped $ZrO_2$ films sliding against a AISI 52100 steel ball display a good wear and friction performance. Best results have been obtained with the 13 mol% $CeO_2$- doped $ZrO_2$ film, which exhibits a friction coefficient as low as 0.22 and a wear-life over 5000 sliding cycles under 1 N load. © 2002 Published by Elsevier Science Ltd and Techna S.r.l.

*Keywords:* Sol–gel; Doped zirconia thin films; Tribological performance

## 1. Introduction

During the last decade, rapidly increased interest was paid to thin film materials, in particular, to wear-resistant coatings [1]. Zirconia has been widely studied due to its superior properties such as high hardness, high wear resistance, high melting point, and chemical stability. Accordingly, zirconia is an important material in high mechanical strength and fracture toughness applications, and it is potentially applied as coatings for wear resistance, corrosion resistance, and heat resistance against oxidation under severe conditions [2–6]. However, it is well known that the phase transformation from the *metastable* tetragonal (*t*) to monoclinic (*m*) phase of crystalline $ZrO_2$ prevents its application over a broad temperature range. The high temperature *t*-$ZrO_2$ phase can be stabilized at room temperature by adding suitable oxide dopants, such as $Y_2O_3$, MgO, CaO, $CeO_2$, $Yb_2O_3$, and NiO to ensure the excellent properties of zirconia ceramics [2,6,7].

The sol-gel process has become a popular method for fabricating ceramic thin films. The main advantage of the sol-gel process is the ability to form inorganic structures at relatively low temperature and to produce thin homogeneous inorganic films on large scale [8]. Although the most common starting materials for the deposition of sol-gel zirconia film until now are zirconium alkoxides [9–13], inorganic zirconium salts also are used as the source of zirconium in preparing a very stable precursor solution at ambient atmosphere [6,14]. Furthermore, inorganic zirconium salts are relatively inexpensive and insensitive to moisture [2,6].

In this paper, we use zirconium oxychloride octahydrate, yttrium nitrate hexahydrate, cerium nitrate hexahydrate, and magnesium chloride hexahydrate as starting materials and anhydrous ethanol as solvent to prepare stable doped zirconia precursor sols. Doped $ZrO_2$ films have been characterized by thermal analysis, morphological analysis and phase analysis. The tribological properties of thin films were also evaluated using a one-way reciprocating tribotester.

## 2. Experimental

### 2.1. Preparation

Doped zirconia thin films of composition 8 mol% $YO_{3/2}$–$ZrO_2$, 8 mol% MgO–$ZrO_2$ and 13 mol%$CeO_2$-$ZrO_2$ (8YSZ, 8MSZ and 13CSZ, respectively) have been prepared with the procedure shown in Fig. 1. The doped $ZrO_2$ sols are transparent and no precipitate is formed at room temperature even after half a year. Si (100) wafers and glass sheets used as substrates were pretreated with piranha solution (volume fraction 3:7 of

* Corresponding author. Fax: +86-931-827-7088.
*E-mail address:* wmliu@1sl.ac.cn (W. Liu).

0272-8842/02/$22.00 © 2002 Published by Elsevier Science Ltd and Techna S.r.l.
PII: S0272-8842(01)00101-8

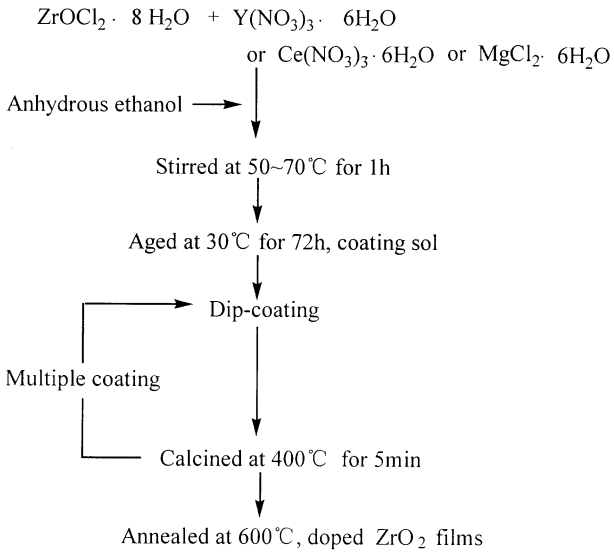


Fig. 1. Flow diagram for the preparation of doped zirconia films.

30% $H_2O_2$ and 98% $H_2SO_4$) at 70 °C for 15–30 min then rinsed with distilled water and anhydrous ethanol. The films were deposited by dip-coating in air at a relatively humidity of 45–55% and withdraw speed of 42.4 cm·min$^{-1}$ obtaining monolayer films about 50 nm thick. The multi-layer films were prepared for XRD analysis.

### 2.2. Characterization

The thermal behavior of the dried gel was investigated by thermogravimetric analysis (TGA; Perkin-Elmer 7 series apparatus, Perkin-Elmer, Norwalk, CT) in nitrogen atmosphere at a scanning rate of 10 °C/min. The chemical binding states in the films were identified using X-ray photoelectron spectroscopy (XPS) performed with a PHI-5702 multifunctional photoelectron spectrometer (Physical Electronics, Minnesota, USA) with a pass energy of 29.35 eV and a Mg $K_\alpha$ line excitation source ($h\nu = 1253.6$ eV). The binding energy of contaminated carbon (C1s: 284.6 eV) was used as the reference. Film microstructure was determined by a D/max-RB X-ray diffractometer (Rigaku Corp., Tokyo, Japan) with Cu $K_\alpha$ radiation at scanning steps of $2\theta = 4°$/min. The XRD spectra were collected for doped $ZrO_2$ films deposited onto a glass sheet. The surface morphology of the films was examined with a SPM-9500 atomic force microscope (AFM; Shimadzu Corp., Kyoto, Japan) using a $Si_3N_4$ probe.

### 2.3. Friction and wear tests

Friction and wear tests were carried out on a one-way reciprocating tester (Model DF-PM, Kyowa Kagaku Corporation, Tokyo, Japan). The counter used in the friction and wear tests was 3 mm diameter AISI 52100 steel ball (composition: 0.95–1.05%C, 1.30–1.65%Cr, 0.15–0.35%Si, 0.20–0.40%Mn, <0.027%P, <0.020%S, <0.30%Ni, and <0.25%Cu) with a hardness of 580 hv. All the tests were conducted under the following conditions: room temperature, relative humidity about 50%, reciprocating distance 9 mm, and sliding speed 120 mm·min$^{-1}$.

## 3. Results and discussion

### 3.1. Mechanism of the sol-gel reaction of inorganic salts

The sol-gel chemical reaction of inorganic salts is more complex than that of metal alkoxides. In general, the inorganic salts in ethanol solution are first transformed into solvate $M_xCl_y \cdot zC_2H_5OH$ or ethoxylate $MCl_a(OC_2H_5)_b$ where the chlorines are partially or fully substituted. After that, in presence of a sufficient amount of water, the solvate or ethoxylate compounds are slowly hydrolyzed to form the hydroxide $M(OH)_n$. Lastly, the ceramic films form by condensation of hydroxides at the proper sintering temperature. Intermolecular condensation of $Zr(OH)_4$ and hydroxides from dopants also occur in the doped films.

### 3.2. Thermal behavior, microstructure and morphology

Fig. 2 presents the TGA curves for doped $ZrO_2$ gel powders formed by heating a sample of the doped sol at 80 °C. As shown in Fig. 2, there are two main stages in the decomposition reaction. About 20% weight is lost below 200 °C due to the evaporation of the water and organic compounds. A second weight loss above 250 °C is attributed to the decomposition of the organometallic compounds that are formed by hydrolysis and condensation during the preparation of the precursor sol. Among them, the second weight loss of 8MSZ is relatively rapid, no weight loss occurs above 500 °C; the weight loss of 8YSZ and 13CSZ is comparatively slow at T > ~250 °C and no weight loss is observed over 600 °C.

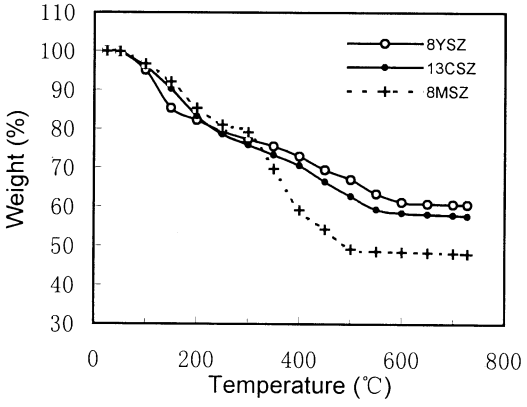


Fig. 2. TGA curves for doped $ZrO_2$ gel powders.

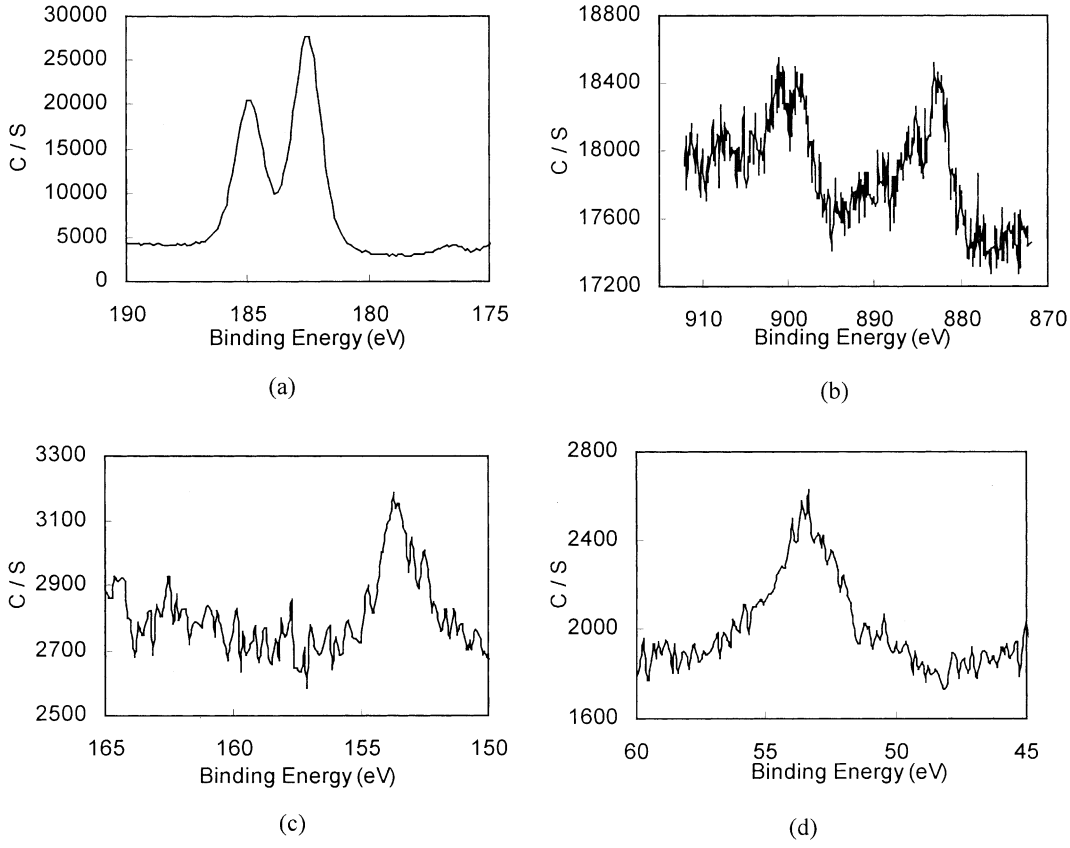


Fig. 3. XPS spectra of (a) Zr3d, (b) Ce3d, (c) Y3d and (d) Mg2p in doped $ZrO_2$ thin films.

XPS spectra of Zr3d, Ce3d, Y3d and Mg2p in doped $ZrO_2$ thin films are shown in Fig. 3. The binding energy of $Zr3d_{5/2}$ is measured at 182.4–182.6 eV and O1s at 530.25 eV, both illustrating the presence of tetragonal $ZrO_2$ [10,15]. This result is consistent with the XRD pattern. Compared with pure sol-gel $ZrO_2$ films [14], a slight shift toward the higher binding energy of Zr3d is observed in doped $ZrO_2$ films, which is due to the difference of the chemical surroundings. From Fig. 3(b–d), it can be seen that the binding energy of $Ce3d_{5/2}$, Y3d and Mg2p is at 882.1, 153.9 and 53.4 eV, respectively. The XPS signals of $Ce3d_{5/2}$ and Mg2p both shift to higher binding energies, while for Y3d shifts to lower binding energy as compared with the XPS signals for pure $CeO_2$, MgO and $Y_2O_3$ [16]. Because of the similarities of structure and cation radius between Zr and Y, a chemical bond of Zr-O-Y can be formed in the doped film. Accordingly, electron transfer from Zr to Y results in the shift to a higher binding energy of $Zr3d_{5/2}$ and to a lower binding energy of the Y3d signal. The XPS signals of Zr3d, Ce3d and Mg2p all shift to higher binding energies and show that 13CSZ and 8MSZ films are mixtures of $ZrO_2$ and $CeO_2$ or MgO.

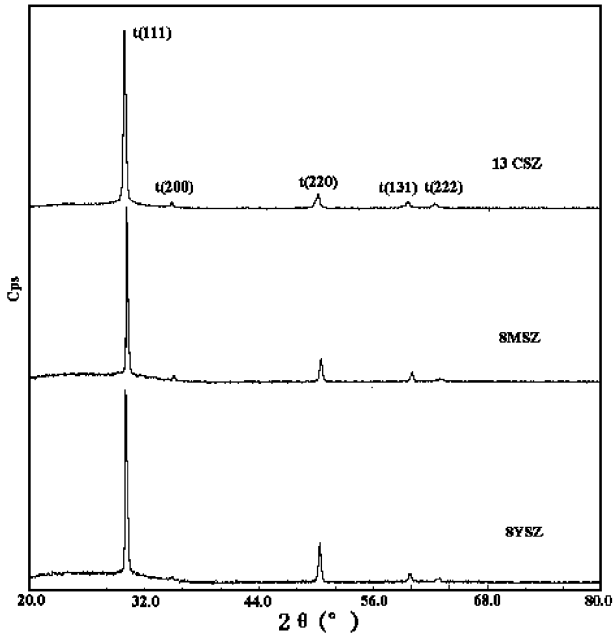


Fig. 4. XRD patterns of doped $ZrO_2$ thin films.

Fig. 4 shows the XRD patterns of doped $ZrO_2$ thin films sintered at 600 °C for 30 min. It can be seen that a complete tetragonal $ZrO_2$ forms for all doped films. The strong peak at $2\theta = 30.2°$ is assigned to the (111) lattice plane whereas the other weak peaks at $2\theta = 35.11$, 50.65, 60.17, and 63.10° may be ascribed to (200), (220), (131), and (222) lattice planes of the tetragonal $ZrO_2$ phase, respectively. This coincides with the low temperature

stabilization of the tetragonal phase. The stabilization of $t$-$ZrO_2$ can be attributed to the structural similarity of the dopants to $ZrO_2$, and to the larger dopant cation radius compared with the $Zr^{4+}$ radius [11]. Another explanation for the stabilization of the tetragonal phase of zirconia in MgO, $Y_2O_3$, or $CeO_2$ doped $ZrO_2$ systems is based on the formation of oxygen vacancies resulting from the presence of divalent and/or trivalent cations [17]. No peak of monoclinic phase is observed in all the doped films. In addition, the doped $ZrO_2$ films show high orientation, with a orientation parameter $\alpha = 0.86$, 0.80 and 0.81 for 13CSZ, 8YSZ and 8MSZ, respectively, ($\alpha$was used to gauge the extent of preferred orientation, where $\alpha_{111} = I_{111}/(I_{111} + I_{200} + I_{220} + I_{131} + I_{222})$ ) while $\alpha = 0.31$ is related to a random powder pattern.

It can be seen from AFM images of the monolayer doped-$ZrO_2$ thin films shown in Fig. 5 (a, b) that the surfaces of 13CSZ and 8YSZ film are compact and uniform, with maximum roughness less than 10 nm. The films are crack-free and consist of nanoscale crystallites. However, the surface of 8MSZ film (in Fig. 5c) is uneven and grooved, giving a maximum roughness higher than 25 nm. The morphology of the doped $ZrO_2$ is related to the decomposition of the gel during sintering. From the TGA curve of 8MSZ in Fig. 2, it can be seen that the decomposition of the 8MSZ gel is faster than the others. During decomposition, gaseous pyrolysate is quickly released, causing surface defects, which affect the mechanical and tribological properties.

### 3.3. Tribological properties

There existed a relatively small amount of literature on friction and wear testing of doped $ZrO_2$ thin films. Yamashita et al. [18] found that unlubricated sputtered $Y_2O_3$- doped $ZrO_2$ thin films having thickness between 20 and 30 nm maintained static friction coefficient less 0.4 for repeated contact start stop (CSS) tests using a read/write head with a force of 0.15 N. Dugger et al. [19] reported that 30 nm thick sputtered $Y_2O_3$-doped $ZrO_2$ thin films lubricated with perfluoropolyester showed greatly improved friction and wear characteristics in humid air compared to dry air or vacuum environments.

Fig. 6 shows the tribological properties of monolayer doped $ZrO_2$ films deposited on Si substrates sliding against AISI 52100 steel ball in dry sliding contact. Fig. 6(a) shows that 13CSZ film sliding against steel ball displays superior tribological properties under low load. A lower friction coefficient of about 0.22 occurs at 1.0 N load, and shows a slight increase with the increase of sliding cycles. Under 0.5 N load, the wear-life is over 5000 sliding cycles, and the friction coefficient is stable

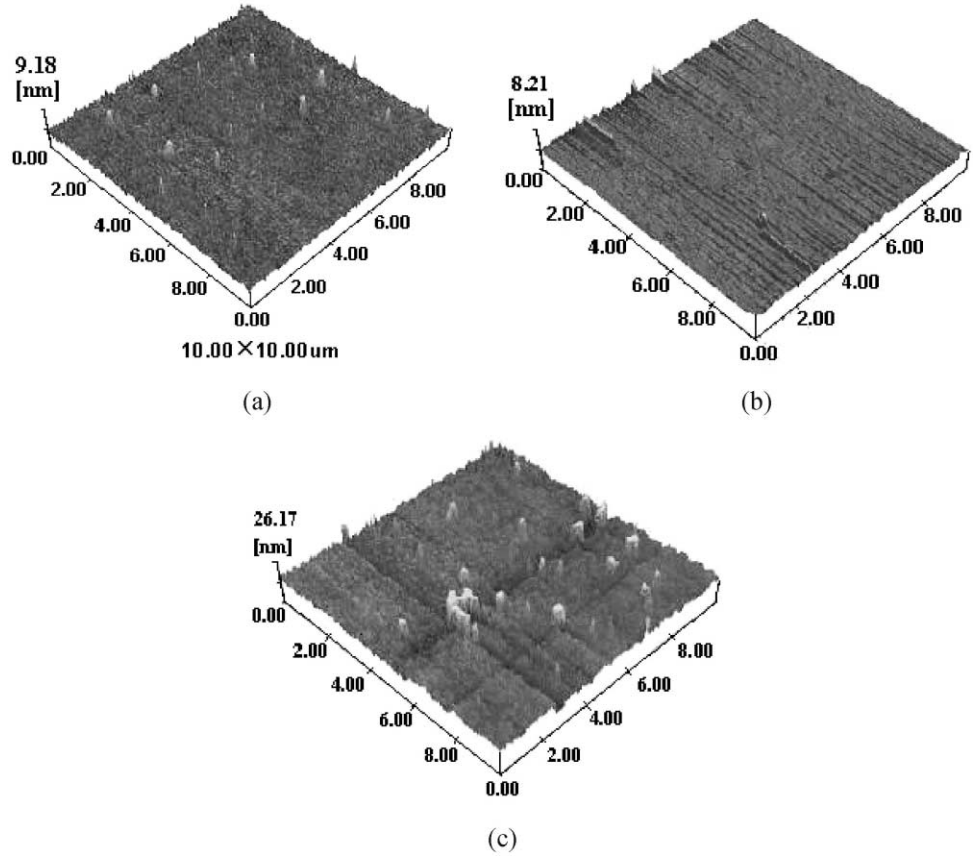


Fig. 5. AFM images of doped $ZrO_2$ thin films: (a) 13CSZ, (b) 8YSZ and (c) 8MSZ.

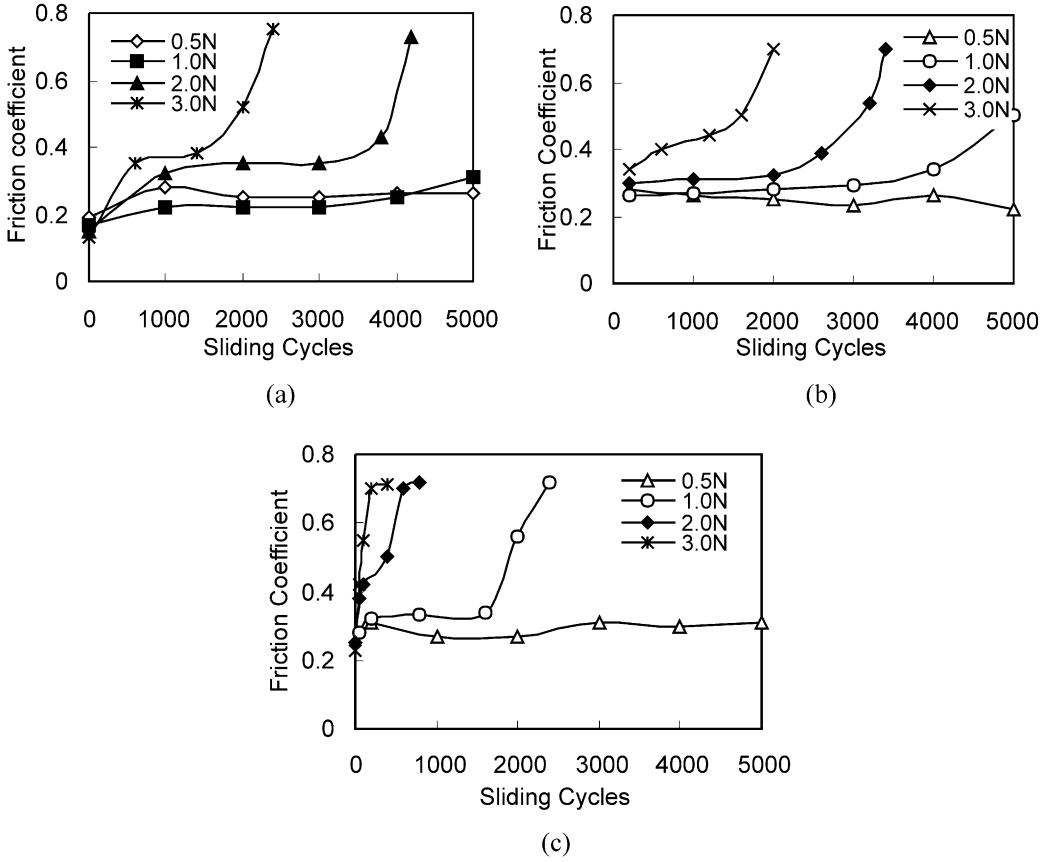


Fig. 6. Friction coefficient as a function of sliding cycles of doped $ZrO_2$ films: (a) 13CSZ, (b) 8YSZ and (c) 8MSZ.

at around 0.25. No wear track is visible on the surface of the film in this case. Therefore, sol-gel $CeO_2$-doped $ZrO_2$ thin films can be potentially applied as ultra-thin lubricating coatings. The friction coefficient and wear of 13CSZ film increase with the load increase in the range of 1.0 N–3.0 N. The friction and wear behavior of the 8YSZ film is similar to that of 13CSZ film as shown in Fig. 6(a, b). Fig. 6(c) gives the friction coefficient *vs.* number of sliding cycles for the 8MSZ film. Compared with 13CSZ and 8YSZ films, the 8MSZ film exhibits lower wear-life and friction reduction performance. A sharp increase of the friction coefficient occurs up to 0.7 around 200 sliding cycles when the load rises to 3 N. The poor tribological properties of 8MSZ film at high load can be attributed to the defect of the surfaces.

## 4. Conclusions

$CeO_2$-, $Y_2O_3$- and MgO-doped $ZrO_2$ thin films have been prepared by the sol-gel process by dip-coating an ethanol solution of zirconium oxychloride octahydrate and the corresponding inorganic dopants. The doped $ZrO_2$ films contain only highly oriented tetragonal phase. The morphology of the $CeO_2$- and $Y_2O_3$-doped $ZrO_2$ films is more uniform and compact as compared with MgO-doped $ZrO_2$ films.

Under low load, doped $ZrO_2$ films sliding against AISI 52100 steel ball display good tribological (wear, friction) performance. The best results are obtained from the 13 mol% $CeO_2$-doped $ZrO_2$ film, which results in friction coefficient of around only 0.22 and wear-life of over 5000 sliding cycles under 1 N load. Because of surface defects, the MgO- doped $ZrO_2$ films show worse tribological properties compared to $CeO_2$- and $Y_2O_3$-doped $ZrO_2$ films.

## Acknowledgements

The authors are thankful to Senior Engineer Shangkui Qi and Engineer Jinfang Zhou at State Key Laboratory of Solid Lubrication of Lanzhou Institute of Chemical Physics, Chinese Academy of Sciences, for their kind help in material characterization. Financial support provided by the National Natural Science Foundation of China (grant No. 59825116) is also acknowledged.

## References

[1] Å.K. Jämting, J.M. Bell, M.V. Swain, L.S. Wielunski, R. Clissold, Measurement of the micro mechanical properties of sol–gel $TiO_2$ films, Thin Solid films 322 (1998) 189–194.

[2] J-S. Lee, T. Matsubara, T. Sei, T. Tsuchiya, Preparation and properties of $Y_2O_3$-doped $ZrO_2$ thin films by sol–gel process, J. Mater. Sci. 32 (1997) 5249–5256.
[3] J.H. Ouyang, S. Sasaki, Unlubricated friction and wear behavior of low-pressure plasma-sprayed $ZrO_2$ coating at elevated temperature, Ceramics International 27 (2001) 251–260.
[4] M.J. Paterson, P.J.K. Paterson, B. Ben-Nissan, The dependence of structure and mechanical properties on film thickness in sol–gel zirconia films, J. Mater. Res. 13 (1998) 388–395.
[5] S.C. Moulzolf, R.J. Lad, P.J. Blau, Microstructural effects on the friction and wear of zirconia films in unlubricated sliding contact, Thin Solid Films 347 (1999) 220–225.
[6] X.S. Ju, P. Huang, N.P. Xu, J. Shi, Development of preparation of porous and dense zirconia membrances, Membr. Sci. Technol. (Chinese) 19 (1999) 11–16.
[7] S. Nakayama, S. Maekawa, T. Sato, Y. Masuda, S. Imai, M. Satamoto, Mechanical properties of ytterbia stabilized zirconia ceramics fabricated from powders prepared by co-precipitation method, Ceramics International 26 (2000) 207–211.
[8] K. Izumi, M. Murakami, T. Deguchi, A. Morita, Zirconia coating on stainless steel sheets from organozirconium compounds, J. Am. Ceram. Soc. 72 (8) (1989) 1465–1468.
[9] S.Y. Bae, H.S. Choi, S.Y. Choi, Y.J. Oh, Sol–gel processing for epitaxial growth of $ZrO_2$ thin films on Si(100) wafers, Ceramics International 26 (2000) 213–214.
[10] R. Brenier, J. Mugnier, E. Mirica, XPS study of amorphous zirconium oxide films prepared by sol–gel, Appl. Surf. Sci. 143 (1999) 85–91.
[11] F. Monte, W. Larsen, D. Mackenzie, Stabilization of tetragonal $ZrO_2$ in $ZrO_2$–$SiO_2$ binary oxides, J. Am. Ceram. Soc. 83 (2000) 628–634.
[12] M.C. Caracoche, P.C. Rivas, M.M. Cervera, Zirconium oxide structure prepared by the sol–gel route: I, the role of the alcoholic solvent, J. Am. Ceram. Soc. 83 (2000) 377–384.
[13] G.L. Tan, X.J. Wu, Electronic conductivity of a $ZrO_2$ thin film as an oxygen sensor, Thin Solid Films 330 (2000) 59–61.
[14] Chen, Y.X., Liu, W.M., Yu, L.G. Characterization and investigation of the tribological properties of sol–gel zirconia thin films, J. Am. Ceram. Soc. (submitted for publication).
[15] C. Urlacher, J. Dumas, J. Serughetti, J. Munoz, Planar $ZrO_2$ waveguides prepared by sol–gel process: structural and optical propertie, J. Sol–Gel Sci. Technol. 8 (1997) 999–1005.
[16] F.M. John, F.S. William, E.S. Peter, D.B. Kennrth, Handbook of X-ray Photoelectroscopy, Physical Electronics, Minnesota, 1995.
[17] V.C. Pandolfelli, J.A. Rodrigues, R. Stevens, Effects of $TiO_2$ addition on the sintering of $TiO_2$–$ZrO_2$ compositions and on the retention of tetragonal phase of zirconia at room temperature, J. Mater. Sci. 26 (1991) 5327–5334.
[18] T. Yamashita, G.L. Chen, J. Shir, T. Chen, Sputtered $ZrO_2$ overcoat with superior corrosion protection and mechanical performance in thin film rigid disk application, IEEE Trans. Magnetics 24 (1988) 2629–2634.
[19] M.T. Dugger, Y.W. Chung, B. Bhushan, W. Rothschild, Wear mechanism of amorphous carbon and zirconia coatings on rigid disk magnetic recording media, Tribol. Trans. 36 (1993) 84–93.